Propagation and refraction of chemical waves generated by local periodic forcing in a reaction-diffusion model

Renwu Zhang
Physical Science Department, Southern Utah University, 351 W. University Blvd., Cedar City, Utah 84720, USA

Lingfa Yang, Anatol M. Zhabotinsky, and Irving R. Epstein*
Department of Chemistry and Volen Center for Complex Systems, MS 015, Brandeis University, Waltham, Massachusetts 02454-9110, USA

(Received 30 March 2007; revised manuscript received 24 May 2007; published 2 July 2007)

We study wave propagation, interaction, and transmission across the boundary between two chemical media in a model of an oscillatory reaction-diffusion medium subjected to local periodic forcing. The forced waves can be either outwardly (OP) or inwardly propagating (IP), depending on the dispersion of the medium. Competition among forced waves, spontaneous spiral waves, and bulk oscillations is studied for both cases. We demonstrate development of a negatively refracted wave train when forced waves traverse the boundary between the OP medium and the IP medium.

DOI: 10.1103/PhysRevE.76.016201 PACS number(s): 82.40.Bj, 47.54.−r, 82.20.−w

I. INTRODUCTION

Local periodic forcing (LPF) of reaction-diffusion systems provides a means of investigating a variety of dynamic questions about spatiotemporal waves and patterns in chemical systems. It is also of interest in developmental biology, medicine and environmental science. For example, a 3D forced wave model has been used to simulate mound formation in *Dictyostelium discoideum* [1]. The effects of LPF have been studied in both oscillatory [2] and excitable [3,4] reaction-diffusion systems. In the latter case, the studies were aimed at development of low-voltage cardiac defibrillators. Low amplitude pacemakers were found to suppress the spiral turbulence, which was considered a model of cardiac fibrillation [3,4]. Periodic drug release via iontophoresis, which can be viewed as a form of LPF, has been suggested as a treatment for cardiac arrhythmias that would have low energy requirements and be capable of modulation in response to changes in arrhythmia activity [5]. In recent decades, the influence of megacities on regional and global pollution has raised concern worldwide [6]. Global air pollution may be related to LPF by chemicals that arise from daily periodic urban activity and are transmitted from cities to remote areas by prevailing winds. Simulation of chemical LPF in a simple chemical medium may shed light on some basic characteristics of the behavior of forced patterns that can enable us to understand, and perhaps to modify, some of the phenomena described above.

When waves propagate from one medium to another, refraction and/or reflection may occur. Refraction and reflection of chemical waves at the interface between two dissipative excitable media have been studied experimentally and theoretically in the Belousov-Zhabotinsky (BZ) reaction-diffusion system. Reflection of chemical trigger waves is quite different from its counterpart in optical or acoustic systems: The angle of reflection is always equal to the critical angle in the dissipative BZ system, in contrast to the specular reflection (equal angles of incidence and reflection) observed in conservative optical systems. Refraction of chemical waves, on the other hand, was found to follow the classical Snell's law in reaction-diffusion systems [7].

Inward propagation of spiral waves in a reaction-diffusion system was recently observed in a water-in-oil AOT microemulsion [8]. In contrast to ordinary concentric or spiral waves, in which waves of chemical activity propagate outward from a source, inwardly rotating spiral or concentric waves propagate toward a central point. Linear stability analysis reveals the physical mechanism behind this difference: in outwardly propagating (OP) waves, the group velocity and the phase velocity have the same sign, while in inwardly propagating (IP) waves, they have opposite signs [9,10].

Oppositely oriented group and phase velocities in chemical waves might give rise to other new phenomena in addition to the anomalous propagation of waves. An obvious case to consider is the refraction of chemical waves at an interface between two reaction-diffusion media. Might such a system exhibit the same abnormal phenomena as seen in optical materials of negative refractive index, where opposite signs of the group and phase velocities result in refraction of light that obeys a *negative* Snell's law, i.e., the refracted light is on the same side of the interface as the incident light? Materials that can have negative refractive index were envisioned as early as 1968 [11]. Only much later were such materials actually manufactured and proposed as a component in novel lenses that could revolutionize modern optical devices [12]. Recently Cao *et al.* [13] have shown that negative refraction can occur at the boundary between two reaction-diffusion media, one of which supports OP and the other supports IP waves.

Here, we use the simple Brusselator model to explore the dynamics of media with OP and IP waves under the influence of LPF in a wide range of forcing frequencies.

*epstein@brandeis.edu; URL: http://hopf.chem.brandeis.edu/

II. METHOD

A reaction-diffusion system may be described by a set of partial differential equations. A general two-variable autonomous model can be written as

$$\frac{\partial u}{\partial t} = f(u,v) + \nabla_r^2 u, \tag{1}$$

$$\frac{\partial v}{\partial t} = g(u,v) + \delta \nabla_r^2 v, \tag{2}$$

where f and g describe the reaction kinetics and the last term in each equation represents diffusion, with δ the ratio of diffusion coefficients, $\delta = D_v/D_u$. Here we choose the abstract Brusselator model [14], in which $f(u,v) = a - (1+b)u + u^2 v$ and $g(u,v) = bu - u^2 v$. We add the LPF term to the first equation:

$$\frac{\partial u}{\partial t} = f(u,v) + \nabla_r^2 u + I(r) A \cos(\omega_{ex} t), \tag{3}$$

$$\frac{\partial v}{\partial t} = g(u,v) + \delta \nabla_r^2 v. \tag{4}$$

where the step function $I(r)$ is 1 inside the pacemaker region and 0 elsewhere, A is the LPF amplitude (we take $A=1.0$), and ω_{ex} is the external forcing frequency.

We deal with media that are oscillatory as the result of a supercritical Hopf bifurcation. In the Brusselator the Hopf instability occurs when $b > b_c^H = 1 + a^2$. With this instability the system is driven away from the steady state $(u_0, v_0) = (a, b/a)$, which results in a limit cycle solution of the ordinary differential equations. In spatially extended systems, this may result in phase-synchronized bulk oscillation (BO), periodic waves or spatiotemporal chaos.

We study the effects of LPF in one- and two-dimensional systems with zero-flux boundary conditions. We employ the direct Euler algorithm with the time step $\Delta t = 5.0 \times 10^{-3}$ time unit (t.u.) and spatial discretization $\Delta x = 5.0 \times 10^{-1}$ space unit (s.u.)

III. RESULTS

A. Effects of LPF on systems that support OP and IP waves

Pacemakers with oscillation frequencies higher than those of the bulk oscillation form target patterns of outwardly propagating waves [15]. Recently patterns consisting of waves propagating toward the center of each spiral have been found in experiment [8], which attracted attention to the phenomenon of inwardly propagating waves. It was shown that such inward propagation took place when the sign of the group velocity of the waves was opposite to that of their phase velocity [8]. Several calculations demonstrated that in such a situation spiral and target patterns of IP waves can occur [9,10,16].

We study here the dynamics of model (1)–(4) beyond the Hopf bifurcation, where the real part of the pair of eigenvalues $\lambda = \alpha \pm i\omega$ is positive, $\alpha > 0$, with nonzero imaginary part, $\omega(k) \neq 0$, the so-called "wave domain." Figure 1 shows two types of dispersion relation in the wave domain for the autonomous Brusselator model, where $\lambda(k) = \alpha(k) + i\omega(k)$ can be calculated analytically by solving the linear stability eigenvalue equation,

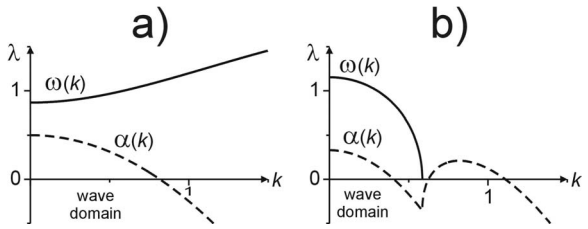

FIG. 1. Dispersion relations for the autonomous Brusselator model: The dominant eigenvalue as a function of wave number, $\lambda(k) = \alpha(k) + i\omega(k)$, calculated from Eqs. (10) and (11). (a) OP waves (parameters: $a=1.0$; $b=3.0$; $D_u=1.0$; $D_v=0.5$); (b) IP waves (parameters: $a=1.2$; $b=3.1$; $D_u=1.0$; $D_v=3.0$).

$$|\mathbf{J} - \lambda \mathbf{I}| = 0 \tag{5}$$

or

$$\lambda^2 - \mathrm{tr}(\mathbf{J})\lambda + \Delta(\mathbf{J}) = 0, \tag{6}$$

where $\mathbf{J}$ is the modified Jacobian matrix,

$$\mathbf{J} = \begin{vmatrix} \frac{\partial f}{\partial u} - k^2 & \frac{\partial f}{\partial v} \\ \frac{\partial g}{\partial u} & \frac{\partial g}{\partial v} - \delta k^2 \end{vmatrix}, \tag{7}$$

with trace

$$\mathrm{tr}(\mathbf{J}) = b - 1 - a^2 - (1+\delta)k^2 \tag{8}$$

and determinant

$$\Delta(\mathbf{J}) = a^2 + [(1-b)\delta + a^2]k^2 + \delta k^4. \tag{9}$$

Solving these equations gives

$$2\alpha(k) = b - 1 - a^2 - (1+\delta)k^2, \tag{10}$$

$$4\omega^2(k) = (b-1-a^2)^2 - 4a^2 + [2(\delta-1)(b-1+a^2)]k^2 + [(1+\delta)^2 - 4\delta]k^4. \tag{11}$$

Figure 1(a) shows the case of positive dispersion, $\partial\omega/\partial k > 0$, which is closely related to normal dispersion in optics and results in the emergence of OP waves. Figure 1(b) illustrates negative dispersion, $\partial\omega/\partial k < 0$, which corresponds to optical anomalous dispersion and leads to generation of IP waves.

Figure 2 shows that in the 1D system pacemakers generate OP waves for a broad range of ω_{ex}/ω_0. There is a wide domain of 1:1 phase locking in the center of this range [Fig. 2(a)]. A spatiotemporal plot for $\omega_{ex}=1.0$ is shown in Fig. 2(c). At pacemaker frequencies below ω_0 the local frequency of oscillations is ω_0, yet the pacemaker still induces fast phase waves [Fig. 2(b), $\omega_{ex}=0.8$]. One can see in this case a transitional process that includes wave splitting. This transition zone occupies a short interval at the left of the frame

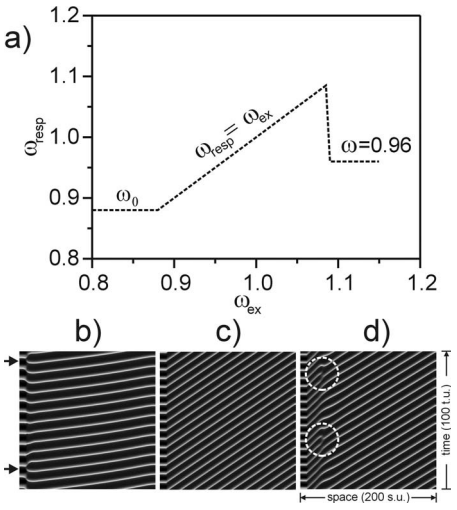

FIG. 2. Effects of LPF on OP waves with parameters in Fig. 1(a). (a) Response to forcing. The middle linear part shows the 1:1 phase-locking of forced waves, while the plateau at the lower left corresponds to fast moving phase waves with the frequency of BO (ω_0=0.88), and the plateau at the upper right corresponds to waves with ω=0.96. (b), (c), and (d) Spatiotemporal plots illustrate these three types of forced waves in a 1D system with zero-flux boundary conditions with ω_{ex}=0.8, 1.0, and 1.1, respectively; A=1.0; size of the pacemakers is 10 s.u. Wave splitting is marked by arrows in (b), 1:1 phase locking OP waves in (c), and local propagation failures are enclosed by dashed circles in (d).

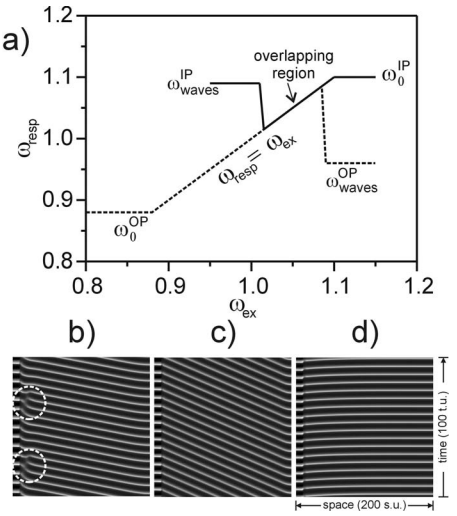

FIG. 3. Effects of LPF on IP waves with parameters as in Fig. 1(b). (a) The solid line shows the effects of forcing on IP waves; for comparison with the dynamics of OP waves, the broken line taken from Fig. 2(a) is also shown. The middle linear part shows 1:1 phase-locking of forced IP waves, overlapping with that of OP waves shown in Fig. 2(a). The plateau to the left of the 1:1 domain corresponds to IP waves with ω=1.09, while the plateau at the right corresponds to bulk oscillation. (b), (c), and (d) Spatiotemporal plots in a 1D system with zero-flux boundary conditions showing three typical responses for IP waves with ω_{ex}=0.95, 1.05, and 1.10, respectively; A=1.0; size of the pacemakers is 10 s.u. (b) Out of phase IP waves with wave splitting episodes enclosed by dashed circles; (c) 1:1 phase locking; (d) fast moving phase waves close to bulk oscillation.

between the pacemaker and the rest of the system. To the right of the 1:1 phase locking domain in Fig. 2(a) there is a domain of OP waves with ω close to (12/11) ω_0. A spatiotemporal plot for ω_{ex}=1.1 is shown in the rightmost panel, Fig. 2(d). In this case, a transitional process results in reduction of the number of propagating waves due to local propagation failure. This transition zone is significantly further away from the pacemaker than in the case of wave splitting at low ω_{ex}.

Figure 3 portrays the behavior of the forced system with IP waves. Figure 3(a) shows the domain of 1:1 phase locking flanked by regions of out of phase IP waves. The corresponding curve from Fig. 2(a) is also plotted as a broken line. Figures 3(b)–3(d), shows the relevant spatiotemporal plots. At pacemaker frequencies below 1.01 the local frequency of oscillations is 1.09, but the pacemaker still induces fast phase waves [Fig. 3(b), ω_{ex}=0.95]. Again the transitional process involves wave splitting, and the transition zone occupies a short interval between the pacemaker and the rest of the system. The central spatiotemporal plot shows 1:1 phase locking with ω_{ex}=1.05. The rightmost plot demonstrates that at $\omega_{ex} \geqslant \omega_0$=1.10 the very fast OP waves are almost indistinguishable from BO.

B. Competition between IP waves and bulk oscillations

Figure 4 shows a 1D system subjected to forcing at its ends with two different frequencies, ω_{left}=1.03 and ω_{right}=1.07, both lower than the BO frequency, ω_0=1.10. The wave numbers are −0.27 (IP1), where the negative sign denotes motion to the left), 0 (BO), and 0.18 (IP2).

IP waves appear at the boundaries of the BO domain and propagate toward the pacemakers. At the same time, the boundaries of the BO domain move in opposite directions, resulting in shrinking of the BO domain. After this domain disappears, the boundary between the two IP wave domains moves toward the pacemaker with *higher* frequency, and eventually the IP waves with the *lower* frequency take over the entire system. The velocity of the domain wall is analogous to the group velocity, and is given by the ratio of the frequency difference over the wavenumber difference of the two neighboring domains, $v_w=(\omega_2-\omega_1)/(k_2-k_1)$. In media with negative dispersion, the pacemaker with the lowest frequency eventually entrains the system, as shown previously in the case of the complex Ginzburg-Landau equation. [17]

C. Suppression of spiral turbulence with LPF

Zhang *et al.* [4] suppressed spiral turbulence in the complex Ginzburg-Landau equation (CGLE) by using a pacemaker to sustain a small spiral wave region at the center of the turbulent area. Here we show that a pacemaker with an appropriate frequency creates a target pattern that gradually eliminates turbulence and occupies the entire system.

In Fig. 5, we create a circular pacemaker of radius 5 s.u. at the center of the system. The forcing frequency is set to ω_{ex}=1.05, which is higher than both the local frequency of

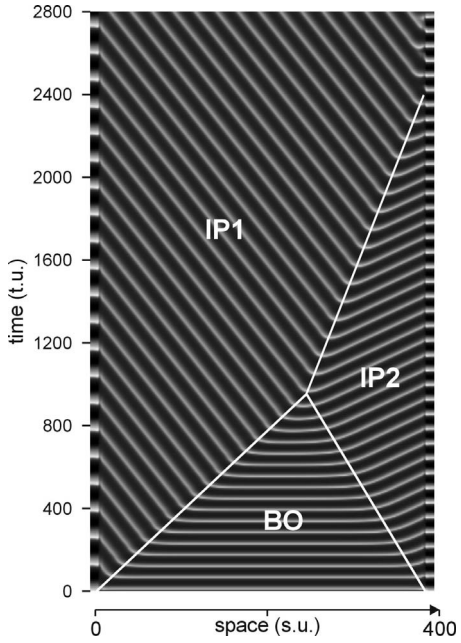

FIG. 4. Competition among two pacemakers and bulk oscillation. The two pacemakers extend from 0 to 10 s.u. and from 390 to 400 s.u. with frequencies 1.03 t.u.$^{-1}$ and 1.07 t.u.$^{-1}$, respectively. Parameters from Fig. 1(b). A stroboscopic plot with sampling frequency 1.03/22 shows the overall dynamics of competition and eventual entrainment of the system. Three domain walls are highlighted, which separate the BO, IP1 and IP2 domains. Their velocities are $v_w=(\omega_2-\omega_1)/(k_2-k_1)=0.26$, -0.17, and 0.09 s.u/t.u..

turbulence ($\omega_{\text{wave}}=0.92$), and that of the bulk mode, $\omega_0=0.89$. The sequence of snapshots in Fig. 5 shows that the turbulence is gradually swept away and ultimately replaced by a target pattern of fast pacing. However, if $\omega_{\text{ex}}<\omega_{\text{wave}}$, the system ignores the forcing, and the turbulence persists.

D. Negative refraction of chemical waves

Refraction of electromagnetic waves involves the change in direction of a wave at an interface when the wave travels

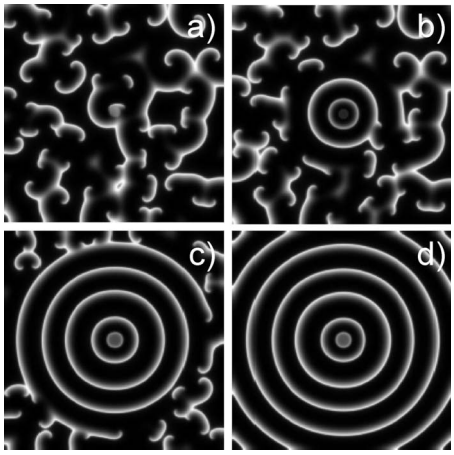

FIG. 5. Spiral waves that develop from random initial conditions at $t=0$ are swept away by a central pacing region. Four snapshots are taken at $t=300$, 640, 1400, and 4300 t.u. System size: 200×200 s.u.; parameters as in Fig. 1(a).

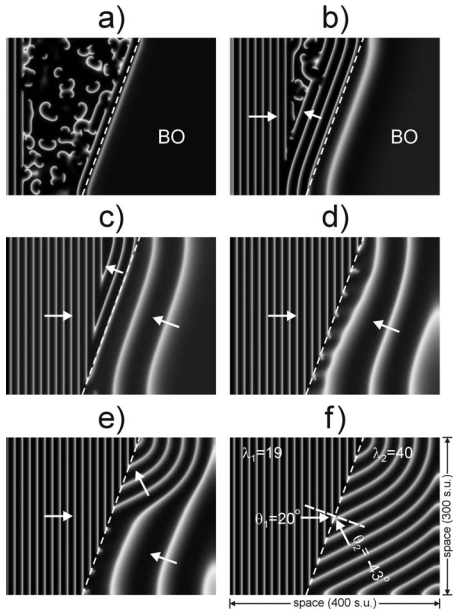

FIG. 6. Evolution of wave patterns in the Brusselator subjected to LPF and establishment of negative refraction of chemical waves. Snapshots (a)–(f) are taken at $t=100$, 500, 1000, 1700, 2200, and 3000 t.u. Negative refraction is seen at the boundary between the two parts of the system in frame (f). Closer to the external boundaries of the system, the refracted wave train is distorted, because the wave fronts are perpendicular to the zero-flux boundaries. System size: 400×300 s.u. Left border (0 to 5 s.u.) is subjected to forcing with frequency 1.05 t.u.$^{-1}$

from one medium into another medium that propagates the wave at a different velocity. At the interface, the wave's phase velocity is altered, but its frequency remains constant, so that phase continuity gives Snell's law

$$n_1 \sin(\theta_1) = n_2 \sin(\theta_2), \tag{12}$$

where θ_1 and θ_2 are the angles of incidence and refraction, respectively, and n_1 and n_2 are the respective indices of refraction. The refractive index of a transparent material was considered to be a positive number until recently, when metamaterials were developed with negative refractive indices [12]. In chemical systems, media which support IP waves behave like metamaterials, and negative refraction may occur at the interface between two media when one supports OP and the other IP waves. This has been demonstrated recently by Cao *et al.* [13].

Figure 6 shows the behavior of a two-dimensional system under LPF. A rectangular system is divided into two equal parts, and the model parameters are set to the values in shown in Fig. 1(a) in the left part of the system and to those shown in Fig. 1(b) in the right part. From random initial conditions, the left part of the system develops spiral turbulence, while the right one generates bulk oscillation. The left border of the system is subjected to LPF, which generates OP waves in the left part, while a wave train emerges at the interface and propagates in the opposite direction [Figs. 6(a) and 6(b)]. Both wave trains have the capability to suppress the spiral turbulence, since they have higher frequency than

that associated with spirals [Fig. 6(b)]. When they meet, the wave train generated by the LPF gradually annihilates the opposite wave train [Figs. 6(c) and 6(d)]. Meanwhile, IP waves generated by the interface emerge in the right half of the system, as shown in Figs. 6(b)–6(d). Figure 6(e) shows the emergence of the refracted wave train. Figure 6(f) shows the stationary pattern of refraction. By measuring the angles and wavelengths, we find that the medium indeed obeys Snell's law (12), but the right side exhibits both a negative index of refraction ($n_2=k_2=\omega/v_p<0$ because the phase velocity is negative for IP waves) and a negative angle of refraction.

An essential criterion for negative refraction to occur is that the 1:1 phase locking region for the IP forced waves must overlap with the phase locking region for the OP forced waves, as highlighted in Fig. 3(a). It is within this overlap region that the forcing frequency must be chosen. Additionally, the LPF frequency must be higher than the frequencies of bulk oscillations and waves in the OP area and lower than those in the IP area so that the waves from the pacemaker can overcome the competition from the other possible modes in both media.

IV. CONCLUSION

It has been experimentally demonstrated that opposite signs of the phase and group velocities of a chemical wave in a reaction-diffusion system give rise to a new type of chemical wave: Inwardly propagating waves [8]. In this paper, we have examined phenomena and properties related to this type of chemical system: The response to external periodic forcing and transmission of the forced waves between media. In normal media, in which the two wave velocities have the same sign, the mode of highest frequency among the external pacing wave, bulk oscillation and intrinsic wave will ultimately dominate. Here, in contrast, when the frequency of an external pacing wave is lower than those of both the natural wave and bulk oscillation, it will finally sweep out any preexisting waves and occupy the entire system. In other words, such chemical systems respond only to external pacing with *lower frequency*.

It seems likely that reaction-diffusion systems possessing opposite signs of their phase and group velocities can support other new phenomena, particularly in configurations involving several components with different properties. Investigation of these fascinating chemical systems may broaden our understanding of chemical wave propagation and transmission in heterogeneous media, with potential implications for materials, biological, and ecological [18] systems as well.

ACKNOWLEDGMENTS

This work was supported by Grant No. CHE-0615507 from the Chemistry Division of the National Science Foundation and by the donors of the Petroleum Research Fund of the American Chemical Society.

[1] Y. Jiang, H. Levine, and J. Glazier, Biophys. J. **75**, 2615 (1998).
[2] J. A. Sherratt, Physica D **82**, 165 (1995).
[3] A. T. Stamp, G. V. Osipov, and J. J. Collins, Chaos **12**, 931 (2002).
[4] H. Zhang, B. Hu, and G. Hu, Phys. Rev. E **68**, 026134 (2003); H. Zhang, B. Hu, G. Hu, Q. Ouyang, and J. Kurths, *ibid.* **66**, 046303 (2002)
[5] V. Labhasetwar, T. Underwood, S. P. Schwendeman, and R. J. Levy, Proc. Natl. Acad. Sci. U.S.A. **92**, 2612 (1995).
[6] H. Akimoto, Science **302**, 1716 (2003).
[7] A. M. Zhabotinsky, M. D. Eager, and I. R. Epstein, Phys. Rev. Lett. **71**, 1526 (1993).
[8] V. K. Vanag and I. R. Epstein, Science **294**, 835 (2001); Phys. Rev. Lett. **87**, 228301 (2001); **88**, 088303 (2002).
[9] L. F. Yang, M. Dolnik, A. M. Zhabotinsky, and I. R. Epstein, J. Chem. Phys. **117**, 7259 (2002).
[10] L. F. Yang and I. R. Epstein, J. Phys. Chem. A **106**, 11676 (2002).
[11] V. Veselago, Sov. Phys. Usp. **10**, 509 (1968).
[12] D. R. Smith, D. Schurig, M. Rosenbluth, S. Schultz, S. Anantha Ramakrishna, and J. B. Pendry, Appl. Phys. Lett. **82**, 1506 (2003); D. R. Smith, J. B. Pendry, and M. C. K. Wiltshire, Science **305**, 788 (2004).
[13] Z. Cao, H. Zhang, and G. Hu, e-print arXiv:cond-mat/0701103.
[14] I. Prigogine and R. Lefever, J. Chem. Phys. **48**, 1695 (1968).
[15] A. N. Zaikin and A. M. Zhabotinsky, Nature (London) **225**, 535 (1970).
[16] Y. F. Gong and D. J. Christini, Phys. Rev. Lett. **90**, 088302 (2003).
[17] M. Hendrey, K. Nam, P. Guzdar, and E. Ott, Phys. Rev. E **62**, 7627 (2000).
[18] J. A. Sherratt and G. J. Lord, Theor Popul. Biol. **71**, 1 (2007).